LAWRENCE
LIVERMORE
NATIONAL
LABORATORY

LLNL-CONF-404878

A Liquid-Cryogen-Free Superconducting Tunnel Junction X-ray Spectrometer for Astrobiology Research at the Synchrotron

S. Friedrich, O. B. Drury, T. Hertrich, J. Hoehne

June 24, 2008

Synchrotron Radiation Instrumentation Conference
Saskatoon, Canada
June 11, 2008 through June 13, 2008

Disclaimer

LLNL-CONF-404878

A Liquid-Cryogen-Free Superconducting Tunnel Junction X-ray Spectrometer for Astrobiology Research at the Synchrotron

Stephan Friedrich, Owen B. Drury

Advanced Detector Group, Lawrence Livermore National Lab, Livermore, CA 94550

Theo Hertrich, Jens Hoehne

VeriCold Technologies, Bahnhofstrasse 18, 85737 Ismaning, Germany

Superconducting tunnel junctions (STJs) are being developed as energy-dispersive soft X-ray detectors, because they combine the high energy resolution of low-temperature detectors with the comparably high count rates of non-thermal devices. We have built a 36-pixel spectrometer based on 200 μm × 200 μm Nb-Al-AlOx-Al-Nb STJs. It offers an energy resolution of ~10 to 20 eV FWHM in the soft X-ray band below 1 keV, a solid angle coverage $\Omega/4\pi \sim 10^{-3}$, and can be operated at total rates up to $\sim 10^6$ counts/s. For STJ operation by non-expert users, we have built a liquid-cryogen-free spectrometer with a mechanical pulse-tube cryocooler and a two-stage adiabatic demagnetization refrigerator. It is fully automated for cooldown to a base temperature of <30 mK in 15 hours, and has a hold time of >3 days between demagnetization cycles for STJ operation at 0.3 K. The STJ spectrometers are used for speciation measurements on dilute samples by fluorescence-detected X-ray absorption spectroscopy, and can achieve sensitivities below 100 ppm. We discuss the spectrometer performance in representative applications on metals in meteorites in the context of geological signatures of biological activity.

PACS numbers: 85.25.Oj, 78.70.Dm, 33.20 Rm, 33.70 Jg, 96.55.+z

Introduction

Cryogenic photon and particle detectors with operating temperatures below 1 K are being developed for scientific and technological applications because of the high energy resolution and high sensitivity that low temperature operation enables. Among the different detector technologies, superconducting tunnel junction (STJ) charge detectors are distinguished by their speed and high count rate capabilities of several 10,000 counts/s per detector pixel, because charge transport in STJs is fast compared to thermal microcalorimeter detectors based on phonon transport. This typically comes at the expense of a lower energy resolution for STJs than for microcalorimeters, since STJ detectors must be operated at $T << T_C$ so that at a given temperature energies to create signal carriers are higher for excess charges than for excess phonons. STJs are therefore preferred in applications that require higher energy resolution than conventional Si(Li) or Ge detectors can offer, and higher count rate capabilities than microcalorimeters. This includes, for example, high-resolution soft X-ray spectroscopy at synchrotron light sources [1].

The widespread use of STJ spectrometers in X-ray spectroscopy depends in part on making this technology available to general users who are typically not experts in low temperature physics. We have therefore built a refrigerator that can attain the required STJ operating temperatures of ~0.5 K or below without the use of cryogenic liquids. The instrument is designed for STJ X-ray operation at the synchrotron, and therefore holds the STJ detector at the end of a cold finger that can be inserted into typical UHV endstations. Here we describe the instrument performance, and illustrate its potential for astrobiology research with an X-ray analysis of metals in a Tagish Lake meteorite sample.

Superconducting Tunnel Junction X-ray Detectors

Superconducting tunnel junctions (STJs) consist of two superconducting electrodes separated by a thin insulating tunnel barrier. X-ray absorption in one of the electrodes excites free excess charges above the superconducting energy gap Δ in proportion to the X-ray energy E_x. As these charges tunnel through the barrier, they generate a temporary current increase that can be directly read out with an FET-based preamplifier at room temperature. The high energy resolution of STJs is due to the fact that the energy $\varepsilon = 1.7\Delta$ to create an excess charge scales with the energy gap Δ. For superconductors, Δ is of order 1 meV and thus a factor ~1000 smaller than in semiconductors, giving rise to an improved energy resolution by a factor $\sqrt{1000} \approx 30$ [2]. Charges can tunnel multiple times ("backtunneling"), each time transfering charge in the *same* direction, until they eventually recombine into the ground state after a time τ_{rec}. This produces an intrinsic gain by a factor $\langle n \rangle = \tau_{rec}/\tau_{tun}$ equal to the average number $\langle n \rangle$ of tunneling events for each charge [3]. In addition, charges in the electrodes at energies $>eV_{bias}$ above the energy gap can also tunnel *against* the bias, this time reducing the signal charge transfer [4]. This process occurs with a probability γ and is suppressed by scattering below eV_{bias}. The signal therefore depends on the relative time scales for tunneling, inelastic scattering and recombination in the electrodes. The associated statistical variations in charge generation and tunneling set the fundamental limit of the energy resolution in STJs to

$$\Delta E_{FWHM} \approx 2.355\sqrt{1.7\Delta \cdot E_x\left(F + 1 + \frac{1}{\langle n \rangle} + \frac{4\gamma(1-\gamma)}{(1-2\gamma)^2}\right)}. \qquad (1)$$

Here $F = 0.2$ is the Fano factor that describes the statistical fluctuations of the initial charge generation process [2], and $1+1/\langle n \rangle$ describes the fluctuations in the average number $\langle n \rangle$ of tunneling events per charge [3]. The γ-dependent term accounts for statistical fluctuations due to

the partitioning of charge transfer with and against the bias [4]. In the limit of strong backtunneling ($\langle n \rangle \rightarrow \infty$) and fast trapping by inelastic scattering ($\gamma \rightarrow 0$), Nb-based STJs (Δ_{Nb} = 1.5 meV) can have an energy resolution between 1.9 eV and 4.3 eV FWHM for photon energies between 0.2 and 1 keV. Experimentally, electronic noise reduces the energy resolution in our small 50 μm × 50 μm Nb-Al-AlOx-Al-Nb STJ detectors to between 4.5 and 8.9 eV FWHM in that band [5], and roughly a factor 2 worse for larger 200 μm × 200 μm STJs [1].

The maximum STJ count rates are determined by the recombination time τ_{rec} that the excess charges remain in the electrodes before they recombine into the superconducting ground state. This recombination time is typically in the microsecond range, and enables STJ detector operation at rates up to several 10,000 counts/s per detector pixel. Our STJs with $\tau_{rec} \sim 3$ μs can be operated at >20,000 counts/s per pixel at maximum energy resolution [6], and up to 100,000 counts/s per pixel for shorter shaping times if the associated degradation in resolution to ~40 eV FWHM is acceptable [1].

Liquid-Cryogen-Free Detector Refrigeration

To make STJ X-ray detector technology available to synchrotron users that are not experts in low-temperature physics, we have built a cryostat that cools the detectors to their operating temperature of 300 mK at the push of a button and without the use of cryogenic liquids (figure 1). Precooling to a temperature of ~3 K is achieved with a mechanical two-stage pulse tube cryocooler based on the compression and expansion of He gas [7]. The main advantage of pulse tubes is that their mechanically vibrating parts such as the rotary valve can be separated from the cold head. This greatly reduces the vibrations at the low-temperature STJ detector stage

and the associated microphonic noise. Their main disadvantage is the comparably high power consumption of the compressor around ~6.5 kW.

Cooling below ~3 K is achieved by isothermal magnetization and adiabatic demagnetization of two paramagnets on two nested stages, which are thermally coupled to the pulse tube cold stage through a heat switch. Most modern adiabatic demagnetization refrigerators (ADRs) use paramagnetic gallium gadolinium garnet $Gd_3Ga_5O_{12}$ (GGG) on the primary "guard stage", and ferric ammonium alum $Fe(NH_4)(SO_4)_2 \times 12\ H_20$ (FAA) on the secondary "detector stage" [8, 9]. Applying an external magnetic field aligns the spins of the paramagnets and lowers their entropy, and the associated heat of magnetization is removed by the pulse tube though the closed heat switch. When the system is equilibrated at ~3 K, the heat switch is opened to isolate the paramagnets thermally. As the magnetic field is lowered slowly, i.e. "adiabatically", keeping the entropy constant, the paramagnets cool the detector cold stage by absorbing heat in their spin system. In our cryostat, the process is fully automated and remote controlled, and can cool down the detector stage close to the FAA ordering temperature of ~26 mK. For operation of our Nb-based STJ X-ray detectors, only a temperature of ~300 mK is required, and the external magnetic field can be controlled to keep the detector stage at 300 mK for >3 days between ~1 hour demagnetization cycles (figure 2).

X-ray Spectroscopy on Meteorites

The development of this STJ X-ray spectrometer is driven by the need for high energy resolution and moderately high speed and detection efficiency for chemical speciation measurements on dilute samples by fluorescence-detected soft X-ray absorption spectroscopy (XAS). Specifically, it is designed for speciation measurements on meteorite samples to correlate

meteorite chemistry with the conditions during fomation and evolution, and potentially identify geological signatures of biological activity. Here we illustrate this approach with X-ray spectra of the Tagish Lake meteorite.

Pieces of a 56-ton meteorite were scattered over a wide area of Canada on January 18, 2000. Many of them landed on the frozen Tagish Lake in the Yukon Territory and northern British Columbia, allowing the recovery of numerous samples in pristine condition and giving the meteorite its name. Neutron activation analysis shows that the meteorite is intermediate in composition between the two most primitive groups of carbonaceous chondrite meteorites, CI and CM [10]. Optical and IR observations of the meteorite's trajectory by U.S. Department of Defense satellites and photos of the residual atmospheric dust clowd have enabled calculations of its path. They trace the origins of the Tagish Lake meteorite to the outer asteroid belt, which is characterized by electromagnetically dark, carbon- and water-rich asteroids. Optical reflectance spectra indicate that the meteorite's parent body is a D-type asteroid, possibly 368 Haidea [11]. These measurements suggest that Tagish Lake is a new type of primitive carbonaceous chondrite meteorite that has possibly been altered by water on its parent body, and may therefore provide new insights about early solar system formation and pre-biotic chemisty.

Figure 3 shows an X-ray fluorescence spectrum of a Tagish Lake specimen for resonant excitation at the energy of 851 eV of the Ni L-edge. The different transition metal L emissions are well resolved, with the Fe L line being strongest as expected [10]. The spectrometer resolution is around ~15 eV FWHM for a count rate of ~10,000 counts/s per pixel. For fluorescence-detected XAS, we scan across the transition metal L-edges and window on the corresponding emission lines. The spectra are normalized by the incident flux and background corrected. Figure 4 shows the Mn and Ni $L_{2,3}$-edges. At the Ni edges, the statistics-limited signal-to-noise ratio is around 70 for a single ~1-hour scan. The L_3 absorption maximum of 853.4 eV and branching ratio, defined as ratio of integrated intensities $L_2/(L_2+L_3)$, of 0.76 suggest that the

nickel exists as high-spin Ni^{2+} in the Tagish Lake meteorite [12]. Even the very weak Mn line can be detected with a sufficiently high signal to noise ratio of ~10 to identify Mn^{2+} as the dominant species from the initial peak at 638 eV, most likely due to $MnCO_3$ [10]. The L_3 edge of the Mn spectum is reduced in magnitude compared to the L_2 edge, most likely due to self-absorption, indiating that Mn exists in the form of small concentrated nodules rather than distributed dilute ions. The detailed analysis of these spectra is currently in progress.

In summary, STJ X-ray spectrometers combine the high energy resolution and broadband efficiency of cryogenic solid state detectors with moderately high count rate capabilities of >20,000 counts/s per pixel. They enable chemcal characterization of dilute samples by fluorescence-detected XAS at low energies when germanium detectors lack energy resolution and grating spectrometers lack efficiency to separate the weak lines of interest from the X-ray background. For STJ operation by non-experts, we have built a liquid-cryogen-free and fully automated cryostat that has a hold time of >3 days at 300 mK with a total of 140 wires connected to the cold stage. Future work will focus on increasing STJ spectrometer sensitivity by increasing the array size to 112 pixels and by replacing the Nb-based STJs with higher efficiency and higher resolution Ta-based detectors.

We thank Matt Morgan for providing the Tagish Lake meteorite sample, and Elke Arenholz for support at ALS beam line 4.0.2. This work was performed under the auspices of the U.S. Department of Energy by Lawrence Livermore National Laboratory under Contract DE-AC52-07NA27344.

References

[1] S. Friedrich, "Cryogenic X-ray detectors for synchrotron science", *J. Synch. Rad*. 13, 159 - 171 (2006)

[2] M. Kurakado, "Possibility of High Resolution Detectors Using Superconducting Tunnel Junctions", *Nucl. Inst. Meth. A* 196, 275 - 277 (1982)

[3] C. A. Mears, S. E. Labov, A. T. Barfknecht, "Energy-Resolving Superconducting X-Ray Detectors with Charge Amplification Due to Multiple Quasiparticle Tunneling", *Appl. Phys. Lett*. 63, 2961 - 2963 (1993)

[4] K. Segall et al., "Noise Mechanisms in Single-Photon Superconducting Tunnel Junction Detectors", *Appl. Phys. Lett*. 76, 3998 - 4000 (2000)

[5] J. B. LeGrand et al., "A Superconducting Tunnel Junction X-Ray Detector with Performance Limited by Statistical Effects", *Appl. Phys. Lett.* 73, 1295 - 1297 (1998)

[6] M. Frank et al., "Energy resolution and high count rate performance of superconducting tunnel junction X-ray spectrometers, *Rev. Sci. Inst*. 69, 25 - 31 (1998)

[7] C. Wang, G. Thummes, C. Heiden, "A two-stage pulse tube cooler operating below 4 K", *Cryogenics* 37, 159 - 164 (1997)

[8] C. Hagmann, P. L. Richards "Two-stage magnetic refrigerator for astronomical applications with reservoir temperatures above 4K", *Cryogenics* 34, 221 - 226 (1994)

[9] S. Friedrich et al., "A superconducting detector endstation for high-resolution energy-dispersive SR-XRF", *Nucl. Inst. Meth. A* 467, 1117 - 1120 (2001)

[10] P. G. Brown et al., "The fall, recovery, orbit, and composition of the Tagish Lake meteorite: a new type of carbonaceous chondrite", *Science* 290, 320 - 325 (2000)

[11] T. Hiroi, M. E. Zolensky, C. M. Pieters, "The Tagish Lake meteorite: A possible sample from a D-type asteroid", *Science* 293, 2234 - 2236 (2001)

[12] H. Wang et al., "L-edge X-ray absorption spectroscopy of some Ni enzymes: probe of Ni electronic structure", *J. El. Spec. Rel. Phen.* 114 - 116, 855 - 863 (2001)

Figure 1: Photograph of the pulse-tube ADR. The STJ detector is held at the end of the cold finger, and the preamplifiers are located in the shielded enclosure on the opposite side. The rotary valve (in the back) between the pulse tube and the compressor is mechanically and electrically isloated from the main body of the instrument.

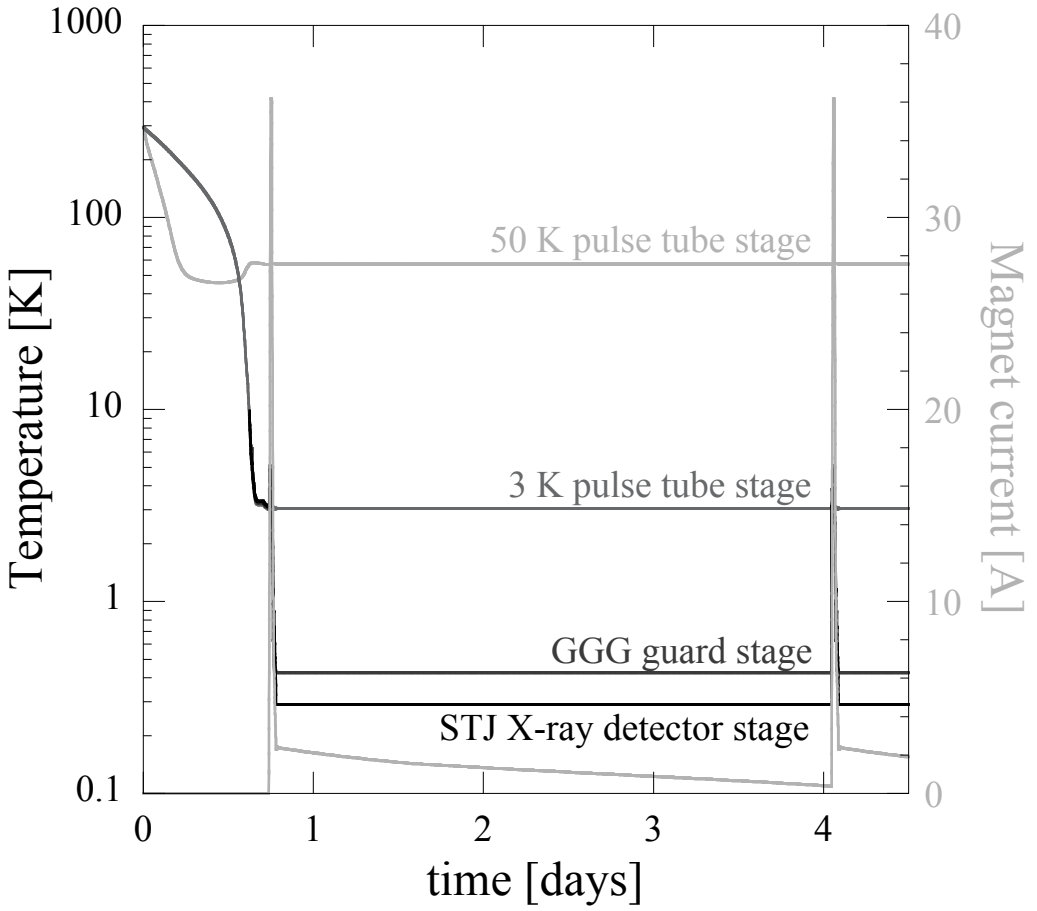

Figure 2: Temperature evolution during an automated cooldown of the cryostat, including the adiabatic demagnetization cycle, and subsequent temperature regulation at 300 mK for >3 days before the next demagnetization cycle.

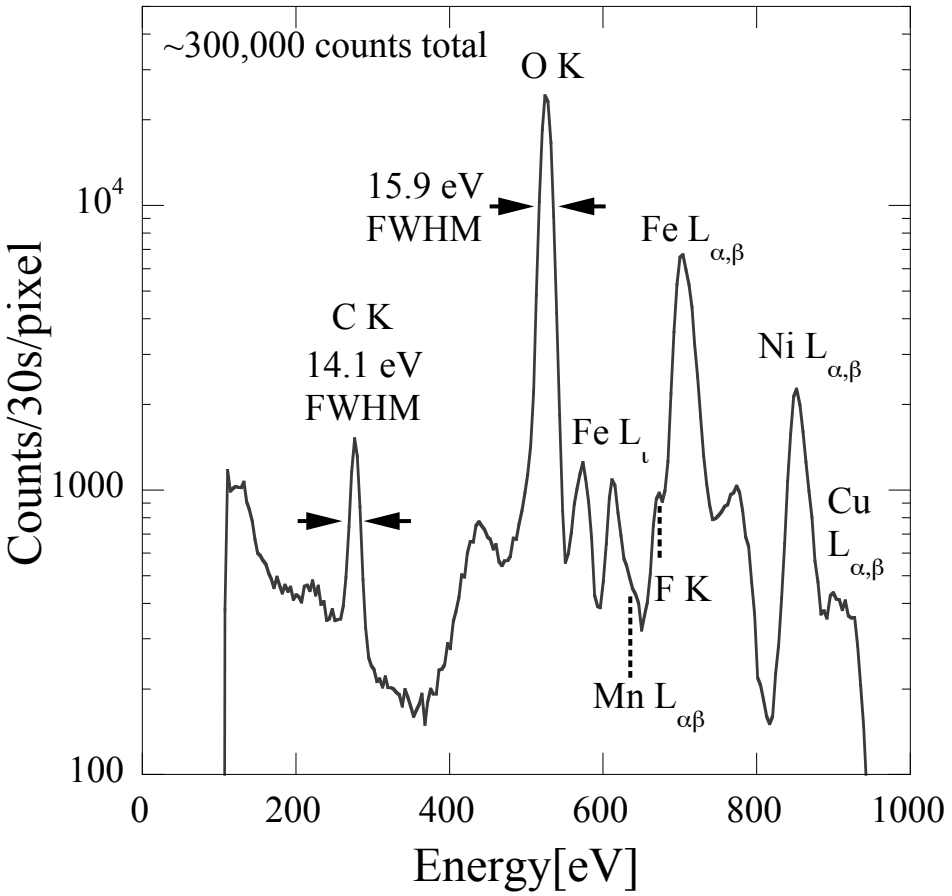

Figure 3: X-ray fluorescence spectrum of a Tagish Lake meteorite sample for resonant excitation at Ni L, taken with a 200 μm × 200 μm STJ detector.

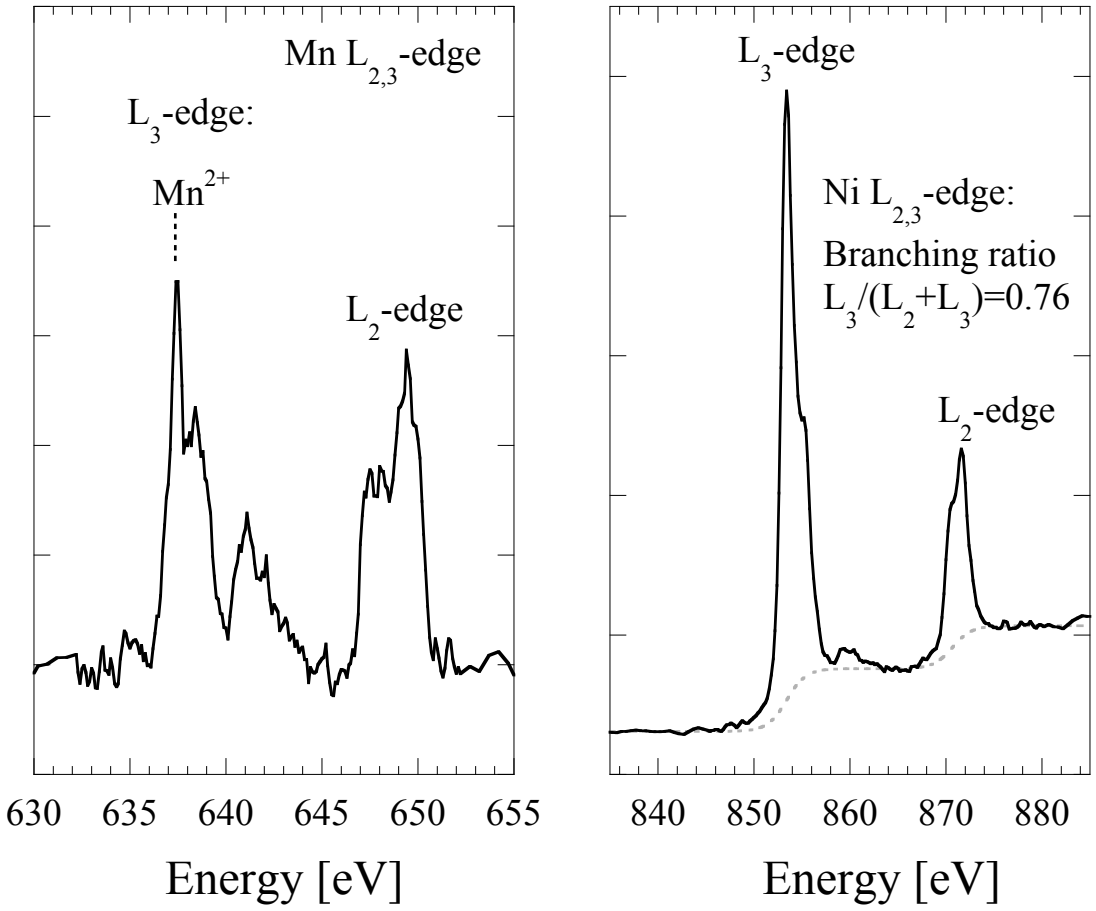

Figure 4: Fluorescence-detected X-ray absorption spectra of the Ni and Mn L-edges of the Tagish Lake meteorite taken with an STJ spectrometer.